Energy 239 (2022) 121915

Contents lists available at ScienceDirect

Energy

journal homepage: www.elsevier.com/locate/energy

Enhanced group method of data handling (GMDH) for permeability prediction based on the modified Levenberg Marquardt technique from well log data

Alvin K. Mulashani [a, b, c], Chuanbo Shen [a, b, *], Baraka M. Nkurlu [b], Christopher N. Mkono [b], Martin Kawamala [b]

[a] Key Laboratory of Tectonics and Petroleum Resources, Ministry of Education, China University of Geosciences, Wuhan, 430074, China
[b] Department of Petroleum Geology, School of Earth Resources, China University of Geosciences, Wuhan, 430074, China
[c] Department of Geoscience and Mining Technology, College of Engineering and Technology, Mbeya University of Science and Technology, Box 131, Mbeya, Tanzania

ARTICLE INFO

Article history:
Received 6 March 2021
Received in revised form
20 August 2021
Accepted 23 August 2021
Available online 30 August 2021

Keywords:
Artificial neural network
permeability
Well logs
Group method of data handling

ABSTRACT

Permeability is the key variable for reservoir characterization used for estimating the flow patterns and volume of hydrocarbons. Modern computer advancement has highlighted the use of machine learning approaches such as group method of data handling (GMDH) in predicting permeability. However, the widely employed GMDH has intrinsic problems in its application. Therefore, the objective of this study is to present an enhanced GMDH based modified Levenberg-Marquardt (LM) as an improved alternative to conventional GMDH in predicting permeability from well logs. The study used natural gamma-ray, standard resolution formation density, limited effective porosity, shale volume of rock, and thermal neutron porosity well logs as input variables. Results show that an enhanced method has a reasonable reduction in processing time with high accuracy. Compared to conventional GMDH and backpropagation neural networks (BPNN), the GMDH-LM used 30% less computation time and performed excellently during training with the least error values of 0.092 and 0.018 for RMSE and MAE. Likewise, good results were observed during testing, obtaining the least error values of 0.679 and 0.056 for RMSE and MAE respectively. The modified generalization performance of GMDH-LM makes it an improved form of GMDH and can be adopted as an improved alternative in predicting permeability.

1. Introduction

Oil and gas are major and valuable commodities in the energy industry which plays an influential role in the global economy as the world's primary source of fuel [1–4]. To guarantee reliable, and fairly priced supplies, oil and gas producers necessitate cheap exploration and production techniques. Permeability plays a significant part in understanding reservoir characteristics, in order to estimate oil and gas reserves available [5,6]. Reservoir permeability is a rock physics parameter that characterizes the difficulty of fluid flowing within the rock, from the reservoir evaluation to the exploration stage and field development. Understanding rock permeability has been among the most essential challenges for petroleum engineers and researchers during the estimation and production of oil/gas [7–10]. Correct prediction of permeability can therefore lead experts to plan and handle more effectively hydrocarbon reserves and their production. Permeability is generally assessed from laboratory rock cores or effectively assessed from well-tested information [11–13]. It could also be estimated indirectly using the data provided by the petrophysical well logs. Despite the existence of diverse parameters such as heterogeneity of reservoirs in several areas, such a precise permeability analysis is necessary, as it is impossible to core some reservoirs [14,15].

The advances of computer technology effectively take into consideration of increasingly regular use of Artificial Intelligence (AI) procedures in everyday geoscience work processes. The utilization of AI keeps on developing in popular inside petroleum geosciences in perspective on regularly developing intricacy and extent of accessible subsurface information data. The successful

* Corresponding author. Key Laboratory of Tectonics and Petroleum Resources, Ministry of Education, China University of Geosciences, Wuhan, 430074, China.
E-mail address: cbshen@cug.edu.cn (C. Shen).

https://doi.org/10.1016/j.energy.2021.121915
0360-5442/

application of artificial intelligence (AI) in hydrocarbon exploration and production in recent years has seen the adoption of machine learning models in predicting permeability from well log data [16,17]. The advantage of machine learning models is their ability to learn and adapt to the dynamics of reservoir conditions such as formation and depositional environment while making use of the entire suite of well logs for a better permeability prediction. Artificial neural network (ANN) has been the predominantly used machine learning method to predict reservoir permeability in studies such as [18–20]. This is because, unlike many other statistical techniques, ANN does not place any constraints on input variables because of its potential ability to model and learn complex and non-linear input-output relationships [21–23]. On the contrary normal ANN models has several disadvantages such as convergence to the minima of the loss function, being prone to overfitting, and computationally intensive procedure that requires much computational time [24–27].

Several researchers have proposed new concepts and improved machine learning algorithms as an alternative to the standard ANN [28–31]. To tackle several drawbacks faced by standard ANN, the group method of data handling (GMDH) approach gives the ability to identify data interrelations, choose an appropriate model or network configuration, and improve the accuracy of existing methods. In complex system modeling, the GMDH was designed to predict, approximate, and identify multivariate system processes [32–34]. The GMDH algorithms are defined by Madala and Ivakhnenko [35] as in each layer, the collection of neurons is connected by a quadratic polynomial that in the next layer generates new neurons. More precisely, the method of conventional GMDH helps to overcome the modeling challenge of the single output of multi-input data [36–38]. Menad et al. [39], clarified that conventional GMDH can also be interpreted to describe nonlinear input-output variable relationships as an algorithm modeling method. GMDH has been applied in many applications of oil and gas engineering. Table 1 shows a summary of some applications of GMDH in the field of oil and gas (see Table 2).

Although conventional GMDH provides a systematic prediction and system modeling, there are still several constraints in its application such as difficulties in finding the optimal partition of data sets and untimely removal of effective parameters which causes minor variations of the model precision [46]. The tendency of producing too complicated network model when dealing with high nonlinear problems due to its two-variable constrained quadratic polynomial (generic architecture). Neurons-weights being determined by a quadratic polynomial is another challenge of conventional GMDH [47,48]. In this case, someone requires to solve the inverse problem during the estimation of coefficients and when calculating the parameter change rate. Therefore, incorrect selection of the variables can, however, lead to an unfit divergence or a case of convergence. Also training conventional GMDH depends on the user's initial assumption which is usually uncertain. As a result, to obtain the global optimum, the user must run numerous trials with several initial assumptions [49].

The present study enhances the applicability of the group method of data handling (GMDH) neural network by using the modified Levenberg Marquardt algorithm (LM) making it an improved GMDH neural network in predicting permeability from well logs data. The modified LM is a hybrid and self-adaptive approach for solving nonlinear least square curve fitting optimization that increases the accuracy of GMDH algorithms by computing its coefficients which ensures fast convergence [50,51]. The GMDH-LM has the ability of self-organizing nature to automatically tune the selected well logs and generate the optimal model structure during training whilst utilizing less computational time. With the least propagation delay, GMDH-LM generates a network and doesn't require background knowledge about the configuration of the final network. The proposed GMDH-LM permeability models' execution is based on network structure as the model coefficients are easily computed on every alteration of a polynomial function of relevant input well logs. To further assess the effectiveness of the GMDH-LM permeability model the result findings were then compared with those obtained by conventional GMDH and ANN of the backpropagation neural network (BPNN). Finally, a variable significance analysis was performed to quantify the impact of each well log parameter on the proposed GMDH-LM model.

2. Data and methods

2.1. Data description

East Africa is vastly growing as a major hub for oil and gas exploration and development. There have been oil finds in Uganda, South Sudan, Tanzania, Kenya, and Mozambique. East Africa is immensely laid in the East African Rift System (EARS) which is an active continental rift zone extending over thousands of kilometers [52,53]. Two main branches of the Eastern Rift Valley are the Western Rift Valley which covers the Albertine Rift stretches farther south to the Lake Malawi gorge, which is situated southwest of Tanzania, and the Eastern Rift Valley, which contains the Main Ethiopian Rift which runs eastward from the Afar Triple Junction, continues south as the Kenyan Rift Valley, also known as the Gregory Rift [54,55].

The Mpyo oil field is found NNE-SSW trending structure identified within the Murchison Falls National Park. the field site is located in the northern chunk of Albertine Graben, along the Eastern Graben Trend, and extends to the north-eastern of the basin margin from the Victoria Nile area [33]. Structurally Mpyo is circumscribed by NE-SW and *N*–S trending major rift faults dipping East with the strata gently dipping towards the South-West [56,57].

Table 1
Applications of GMDH in oil and gas field.

Reference(s)	Application	Notes
[33]	Reservoir Permeability prediction	GMDH neural network was used to successfully predict permeability from well logs
[40]	Prediction of hydrate formation temperature	Hybrid GMDH was used in the prediction of hydrate formation temperature of a wide range of natural gas mixtures including sweet and sour gas.
[41]	Prediction of time series oilfield production.	Modified GMDH used to forecast time series of oilfield production using reservoir parameters.
[42]	Prediction of airflow	A novel integrated GMDH was developed and applied to estimate air demand on the spillway using flow parameters.
[43]	Methane adsorption capacity modeling and prediction in shale gas	The GMDH was utilized to provide accurate and reliable explicit mathematical expressions for predicting methane adsorption.
[44]	Prediction of formation permeability	GMDH was used to estimate the formation permeability of the heterogeneous carbonate oil reservoir from petrophysical properties.
[45]	Stand Pipe Pressure (SPP) prediction	The extended GMDH was used to predict the Stand Pipe Pressure (SPP in real-time as a function of mudflow from drilling parameters.

Table 2
Statistical features of the used data.

Well 1					
Statistical features	TNPH (v/v)	SGR (API)	VSH (pU)	PHIE (%)	RHOZ (g/cc)
Minimum	0.123	8.425	0.0016	0.017	1.683
Maximum	1.615	74.87	0.912	0.451	4.097
Average	0.494	38.18	0.268	0.195	2.338
Standard Deviation	0.311	12.13	0.191	0.099	0.410
Range	0.382	27.58	0.425	0.25	1.83
Well 2					
Statistical features	TNPH (v/v)	SGR (API)	VSH (pU)	PHIE (%)	RHOZ (g/cc)
Minimum	0.123	16.212	0.020	0.009	1.683
Maximum	1.616	74.875	0.912	0.372	4.097
Average	0.741	44.568	0.346	0.188	2.481
Standard Deviation	0.348	11.207	0.219	0.099	0.587
Range	1.492	58.663	0.892	0.363	2.414
Well 3					
Statistical features	TNPH (v/v)	SGR (API)	VSH (pU)	PHIE (%)	RHOZ (g/cc)
Minimum	0.252	13.699	0.014	0.009	1.927
Maximum	1.035	72.729	0.911	0.372	3.486
Average	0.376	42.145	0.309	0.188	2.169
Standard Deviation	0.101	15.535	0.240	0.098	0.128
Range	0.783	59.030	0.897	0.363	1.559

Also, the Mpyo structure is located southeast of the Jobi/Rii discovery and about the Jobi East structure to the north Fig. 1(a).

The study area is believed to be dominated by clastic sediments aged from tertiary to quaternary. Major lithologies are believed to be climatically controlled with clay and sand deposition episodes dominate during water and dryer season respectively. Semanya formation is dominated by very fine to very coarse sediments with occasional gravel. Upper Paraa Formation is a loose grain of sand with interbedded claystone. Lower Paraa Formation is dominated by red-brown to brown claystone with rare sand. It is also interbedded with light to green-grey claystone with a minor silty and sandy appearance. Pacego Formation is characterized by coarsening upward sand at the top which is poorly sorted, very fine to medium, sub-angular to round, elongate to sub-spherical. Below is claystone with silt/sand interbeds. Wangkwar contains the reservoir sands interbedded with siltstones and claystone. The formation has varied characteristics, it contains interbedded claystone, siltstone, and sandstone with an overall fining downward. Since it is a fining downward formation, the claystone dominance increases as the depth increases. The lower zone represents the weathered basement (mix of clay and sand). Fig. 1(b) describes the stratigraphic diagram of the formations under study.

This study included three wells, well-1, well-2, and well-3. These wells are found in the west arm of the EAR valley and the North of Lake Albert in the Mpyo oilfield. They also sit in the area in the southern part of Job east discovery and the eastern part of Ondyek 1.356 well log data from wells 1 and 2 were used for model training. The trained models were tested using 274 permeability data and well log data from well-3. For the network development, the well log inputs of natural gamma-ray (SGR), Standard Resolution Formation Density (RHOZ), limited effective porosity (PHIE), shale volume of rock (VSH), and thermal neutron porosity (TNPH), were selected (Fig. 2). Using the min-max standard method the permeability data and entire well logs were normalized so that the artificial intelligent models could interpret and treat the output and input data unbiasedly Equation (1) [58,59].

$$y_i^{'} = \left[\frac{y_i - y_{\min}}{y_{\max} - y_{\min}}\right] \tag{1}$$

Where y_i' is the normalized value of y_i, y_i is the original value of the parameter, $y_{\max}$ and $y_{\min}$ are the maximum and the minimum values of y_i, respectively.

2.2. Backpropagation neural network (BPNN)

In determine the output network values of permeability using backpropagation neural network (BPNN), the inputs used in this present study were the well logs of SGR, RHOZ, PHIE, VSH, and TNPH. To assign non-linearity to the network, the linear function was adopted for the output nodes, whereas the hyperbolic tangent activation function became defined for the hidden layers, Equation (2) [60–62].

$$f(z) = \tanh(z) = \frac{2}{1 - e^{-2z}} - 1 \tag{2}$$

Whereas, total weighted inputs are represented by z. It is worth noting that BPNN training can be defined as the non-linear optimization problem, given by Equation 3

$$r^* = \arg\min U(r) \tag{3}$$

where $U(r)$ is the error function and r is the weight matrix. The objective of training the network is to determine the optimum weight connection (r^*) that lessens $U(r)$ in such a way that the predicted outputs values of BPNN adhere to the desired output [63]. This $U(r)$ is estimated at any point of r as Equation 4

$$U(r) = \sum_n U_n(r) \tag{4}$$

where $U_n\ (r)$ is the output error and n is the number of training cases for each case n. $U_n(r)$ is defined mathematically by Equation (5).

$$U_n\,(r\,) = \frac{1}{2}\sum_j \left(y_{nj} - \hat{y}_{nj}\,(r\,)\right)^2 \tag{5}$$

Where $\hat{y}_{nj}\ (r)$ and y_{nj} are predicted and targeted output values of the network for nth sample and jth output neuron respectively. Hence, a simplified objective function which is to be minimized Equation (6) can be obtained by substituting Equation (5) into Equation 4

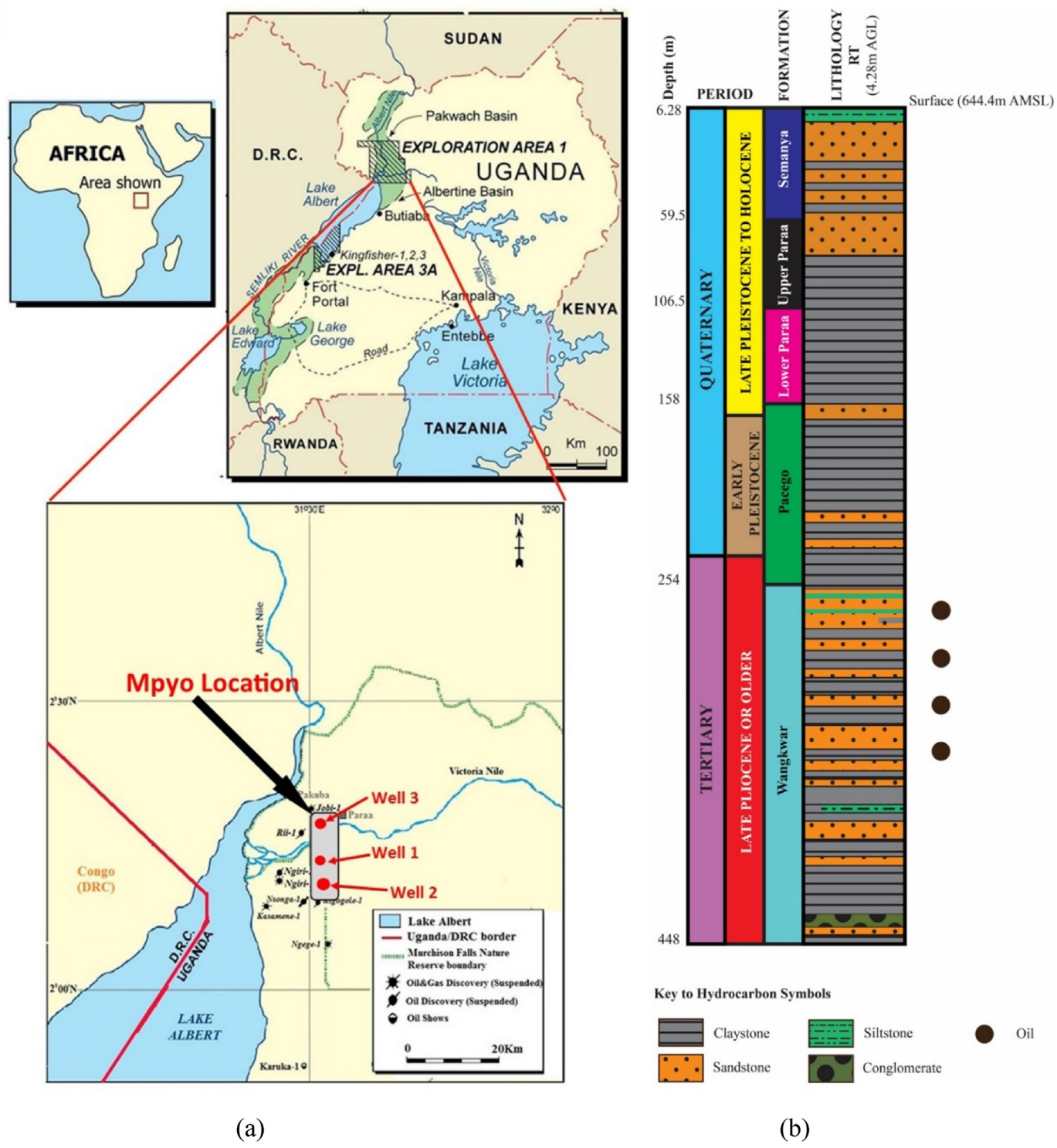

Fig. 1. (a) Regional Map of the Mpyo oil field (b) The stratigraphic diagram of the formations understudy.

$$U(r) = \frac{1}{2}\sum_{n}\sum_{j}\left(y_{nj} - \hat{y}_{nj}(r)\right)^{2} \tag{6}$$

The training progression continues through modifying the weight of the output neurons and after that progresses to the data of the input before the error function hits a value that will be regarded as an appropriate value [64]. This weight adjustment is performed, through several numerical optimization algorithms.

2.3. Conventional group method of data handling (GMDH-C)

The objective of the conventional GMDH model is characterized

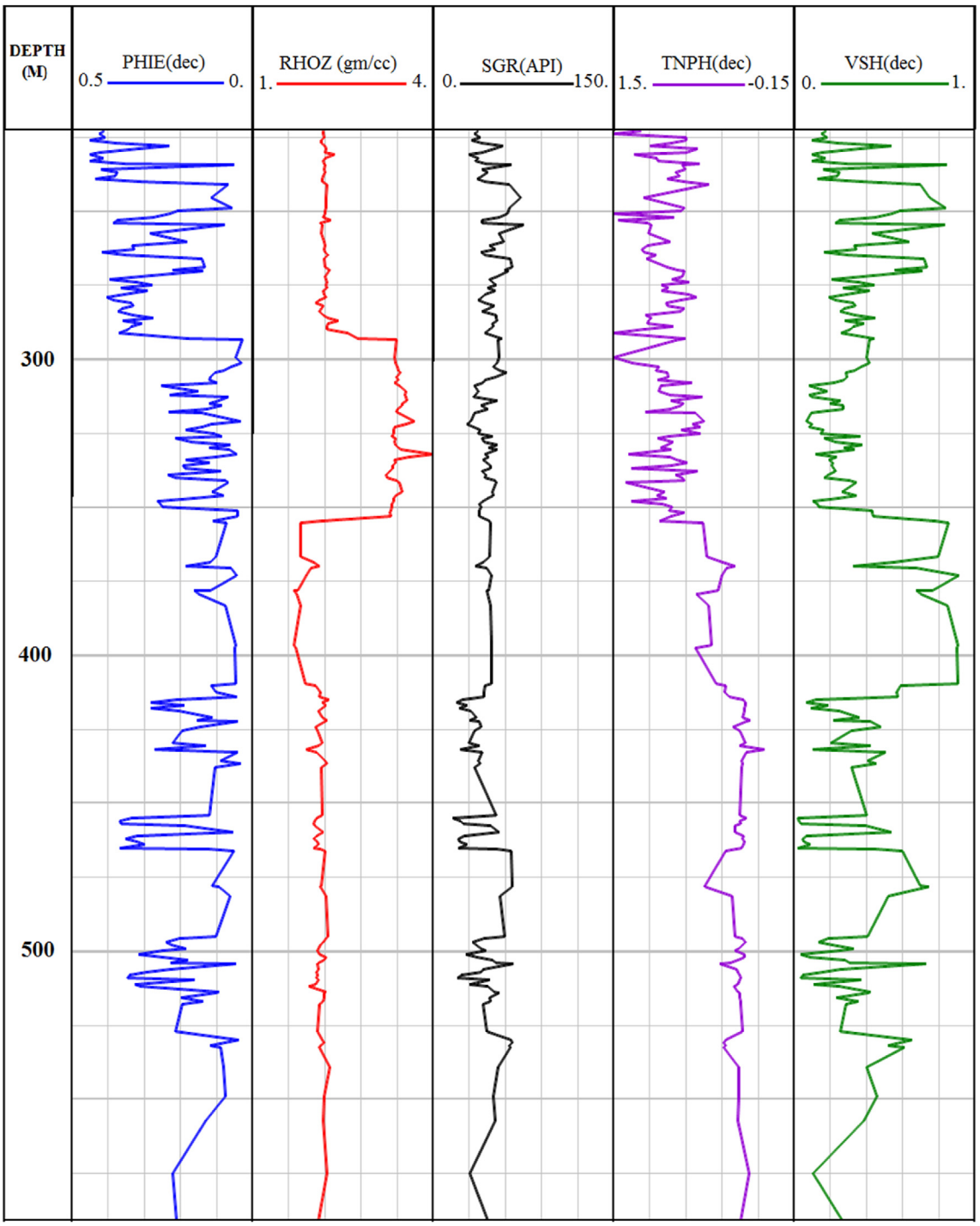

Fig. 2. Sample geophysical well logs of limited effective porosity (PHIE), (RHOZ), natural gamma ray (SGR), rock's shale volume (VSH), and thermal neutron porosity (TNPH).

by finding a function $\widehat{F} = \widehat{y}$ that could be applied as an approximation function on behalf of real function $F = y$, to predict the values of output $\widehat{y}$ for the certain input system vector $(X) = F(x_1, x_2, x_3, \ldots x_n)$, as close as real output y (Permeability) [33]. The GMDH network structure with y_n output and x_n model input is shown in Fig. 3.

Thus, the number of 'N' given the observation of numerous inputs having data pairs of output y such that [32],

$$y = F(x_{i1}, x_{i2}, x_{i3}, \ldots..., x_{in}) \text{here} (i = 1, 2, \ldots, N) \quad (7)$$

Now it is easy when training the GMDH network to forecast the approximated variable of output $\widehat{y}$ for any assumed system of input (X) that is

$$\widehat{y} = \widehat{F}(x_{i1}, x_{i2}, x_{i3}, \ldots..., x_{in}) \text{ for } (i = 1, 2, \ldots, N) \quad (8)$$

Mathematically, the GMDH creates a general relation between output and input variables, both to be considered as a reference point [65]. The challenge here is to govern and determine the GMDH network that will make a square of the difference between

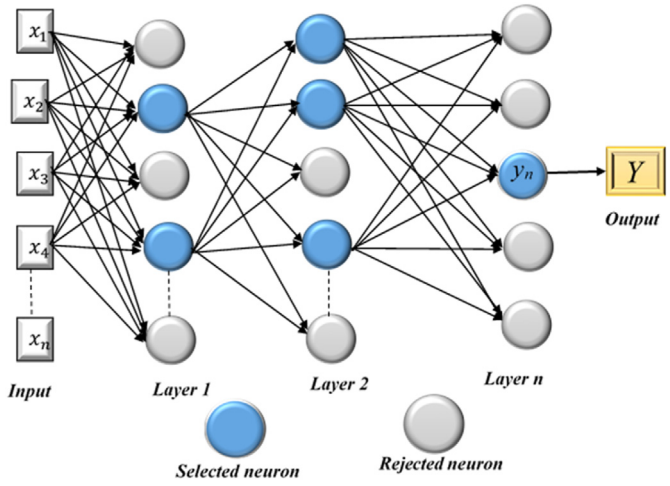

Fig. 3. Shows the conventional GMDH network structure having n inputs.

actual output (y) and the estimated output $\hat{y}$ is minimized,

$$\sum_{i=1}^{N}[\hat{y}-y_i]^2 \sim min. \tag{9}$$

In general, the network connection between the output and input parameters can be described through the complex discrete series formula in the form of Volterra functional, referred to as Kolmogorov–Gabor polynomial Equation (10).

$$y = a_o + \sum_{i=1}^{n} a_i x_i + \sum_{i=1}^{n}\sum_{j=1}^{n} a_{ij}x_{ij} + \sum_{i=1}^{n}\sum_{j=1}^{n}\sum_{k=1}^{n} a_{ijk}x_i x_j x_k + \ldots \tag{10}$$

Whereby n denotes the number of the inputs, x denotes the system input and a is the coefficient.

In general, in the form of partial quadratic equations containing only two neurons, the discrete polynomial proposed in Equation (10) above is applicable:

$$\hat{y} = a_0 + a_1 x_i + a_2 x_j + a_3 x_i x_j + a_4 x_i^2 + a_5 x_j^2 \tag{11}$$

Equation (10) is developed in a link of network neurons using the description of partial quadratic iteratively and is the complete mathematical relation between output and input through regression method [66], the coefficient a_i Equation (11), can be determined to lessen the discrepancy between the predicted output $\hat{y}$ and desired output y in every pair of the input values, x_i,x_j. In this, the tree of polynomials tends to be formed using the form of a quadratic Equation (11) in which the function coefficients are obtained and gained in the least-squares approach [67]. The coefficient of each quadratic equation, $\hat{y}_i$ for the output of the entire input-output data pair set can be found for an optional fit as follows:

$$MSE = \frac{1}{N}\sum_{i=1}^{N}(y_i - \hat{y}_i)^2 \sim min \tag{12}$$

All the probabilities of two parameters which are independent and accessible from entire n input parameters are drawn in the general formula of the GMDH algorithm to create the regression polynomial like that of Equation (12), which matches the dependent outcomes $(y_i, i = 1,2,3\ldots,N)$ in the sense of least square [68,69].

For the development of the regression polynomial in sense of Equation (11), out of the general n input values, the whole series of possibilities for two different values is assumed to be the best way to construct the first dependent targets $(y_i, i = 1,2,3\ldots,N)$ regarded in the sense of least-square [70]. As a consequence, $\binom{n}{2} = n(n-1)/2$ numbers of the neuron can be created at the before hidden FFN level taken from the observations $y_i; x_{pi}, x_{qi} (i = 1,2,3\ldots,N)$ for different p: q 1; 2; 3, … values [71]. Realistically, this shows that N data triples $y_i; x_{pi}, x_{qi}\ldots; (i = 1,2,3\ldots,N)$ from observations employing p; q A (1; 2; 3 ….); in the form Equation (13) [72,73].

$$\begin{bmatrix} x_{ip} & x_{1q} & : & y_1 \\ x_{2p} & x_{2q} & : & y_2 \\ \cdots & \cdots & \cdots & \cdots \\ x_{Np} & x_{Np} & : & y_N \end{bmatrix} \tag{13}$$

The following equation of matrix is formed from every row of N by using quadratic sub-expression in form of Equation (11).

$$A_a = Y \tag{14}$$

$$a = [a_0, a_{,1} a_2, a_3, a_4, a_5] \tag{15}$$

$$Y = [y_1, y_2, y_3, \ldots y_N]^T \tag{16}$$

It could be easily observed that:

$$A = \begin{bmatrix} 1 & x_{1p} & x_{1q} & x_{1p}x_{1q} & x_{1p}^2 & x_{1q}^2 \\ 1 & x_{2p} & x_{2q} & x_{2p}x_{2q} & x_{2p}^2 & x_{2q}^2 \\ \cdots & \cdots & \cdots & \cdots & \cdots & \cdots \\ 1 & x_{Np} & x_{Nq} & x_{Np}x_{Nq} & x_{Np}^2 & x_{Nq}^2 \end{bmatrix} \tag{17}$$

The normal solutions for equations can be generated by the least square technique in the form of:

$$a = \left(A^T A\right)^{-1} A^T Y \tag{18}$$

2.4. GMDH model based on modified Levenberg-Marquardt (GMDH-LM)

The nonlinear algebraic equation for the general determined system is given by Equation (20) [74–76].

$$f(a,b) = y \Rightarrow f(a,b) - y = w \tag{20}$$

Where as y is output required while b is unknown constant. Its approach is achieved by minimizing $w_2^2 = w^T w$ in the sense of optimal least squared technique [77]. Here zero values of partial derivatives of w_2^2 due to unidentified coefficients b, are the important conditions for the best solution which is;

$$\frac{\partial w_2^2}{\partial b} = 2\frac{\partial w^T}{\partial b} r = 2J^T w = 2v \tag{21}$$

Here J, elements which are known as the Jacobian matrix, are $j_{ij} = \frac{\partial_{wj}}{\partial_{bj}}$. Vector v must be equal to zero vector for the best solution of b^* point [78]. It is pursued after nth iterations in the form

$$b^{(n+1)} = b^{(n)} + \Delta b^{(n)} \tag{22}$$

Let residual $w(b)$ be smooth functions, and then it holds:

$$w^{(n+1)} = w^{n} + \frac{\partial w^{n}}{\partial b^{n}} \Delta b^{(n)} + \ldots. \tag{23}$$

After some techniques of manipulations, the equation for the expression increase following the form of Equation 24

$$A^{(n)} \Delta b^{(n)} - J^{(n)^{T}} w^{(n+1)} = -v^{(n)} \tag{24}$$

The λ^{n+1} values differ depending on the actions of the iteration process. For slow, stable iteration convergence, the new value $\lambda^{(n+1)} = \lambda^{(n)}/\upsilon$ is set to speed up the process. If a sign of divergence is noted, the value will be changed to $\lambda^{(n+1)} = \lambda^{(n)}\upsilon$. The normal value of υ is between 2 and 10, respectively. Fletcher significantly improved Marquardt's technique of adaptation to λ [79,80]. Moreover, in the current iteration process, a new quotient R that expresses how the predicted sum of squares agrees with the real one is introduced. If R falls between the preset limits (R_{lo}, R_{hi}), the iteration parameters do not change, otherwise, the λ and υ changes will follow. If $R > R_{\mathrm{hi}}$, the value of λ is halved. If λ is lower than a critical value λ_b, it will be cleared, allowing the next iteration to continue as in the Newton process [81]. If $R < R_{\mathrm{lo}}$, the parameter υ is set so that it holds $2 \leq \upsilon \leq 10$, and if λ is zero, λ_b and λ are changed. The stages involved in the model development include:

Step 1: The original well log and core permeability data are standardized and then divided by the arbitrary drawing sample method into training and testing data sets. The training set is used to train the GMDH−LM model, whereas the testing set is used to judge how well the model predicts the predestined data.

Step 2. Identify the initial conditions for creating the GMDH-LM structure such as the maximum input variables received at each node, the maximum number of layers and nodes per each layer, modified LM parameters, polynomial type, and the stopping criterion.

Step 3: Estimate the variable coefficients of every node: In the selection stage, through combining every two nodes of the previous layer, the candidate models are generated to get the new input nodes, which refer to the best solutions, recognized according to their fitness. The unknown parameters are estimated on the training set by external criterion (least squares). This process is implemented repeatedly for all nodes as (i). With the initial weights and biases generated randomly, Calculate the Jacobian J and the total sum of squared error. (ii) Update the weights Δw and biases Δb as directed by Equation (24). (iii) With the new weights and biases, recalculate the total sum of squared error for all inputs (iv). If the total error is not satisfactory, repeat from sub-step (ii) by increasing λ and recalculate biases and weights, otherwise calculate the outputs of the neurons.

Step 4: The selected intermediate neurons survived, and they are used as the inputs for the next layer to create the new generation of neurons of the model while the non-selected neurons are abandoned.

Step 5; The modeling process can be terminated once the stopping criterion is met. When the stopping criterion is not achieved, Steps 2−4 are repeated until the optimal complexity model is automatically obtained based on the self-organizing and metaheuristic nature of the GMDH-LM algorithm. The testing data set is applied to validate the model.

Step 6. To obtain the final GMDH-LM model, the path of the neurons that corresponds to the lowest error in every layer is tracked back. Following the evolution process, the candidate with the highest performance in the ending alteration is adopted as the network's final structure. The predicted value of the current query point is the output of the selected network. A graphical illustration steps of the GMDH-LM model development for permeability prediction is presented in Fig. 4.

3. Results and discussion

3.1. GMDH-LM model development

GMDH-LM neural network model based Levenberg−Marquardt was coded and executed in the MATLAB R2020a. The developed GMDH-LM output consisted of two hidden layers in which the first layer has three neurons which are represented by z_1, z_2, *and* z_3 whereas the second hidden has two neurons represented as f_1 and f_2 with one output layer which is denoted as y. As stated earlier, the only statistical responsibility for comparing the input and output layer is for these unitless hidden neurons. After a series of adjustment progressions, this configuration was achieved by observing the real presentation of the GMDH-LM network until the desired network structure was achieved. Fig. 5 shows in detail the built permeability model. The model network layers equations required to generate the prediction of permeability are given in Table 3.

Where x_4 is thermal neutron porosity (TNPH), x_1 is natural gamma-ray (SGR), x_3 is Limited effective porosity (PHIE), and Standard resolution formation density (RHOZ) is represented by x_2

3.2. Performance indicators

GMDH-LM, conventional GMDH, and backpropagation neural network (BPNN) models were implemented in MATLAB R2020a on ADM A8-6410APU, with Windows 10 operating system. The results from the predictive developed permeability models were fairly compared using correlation coefficient (R) mean absolute error (MAE) and relative root mean square error (RMSE) as a statistical indicator. A correlation coefficient (R) close to 1 signifies the best model performance. On the contrary, if the MAE and RMSE value approaches zero during the model's comparison, indicates that the model is an accepted predictor. Mathematical expressions for R, MAE, and RMSE are provided in Equation (25) 26, and 27 [19,23,82].

$$R = \frac{\sum_{i=1}^{N}(y_i - \overline{y})(Y_i - \overline{Y}_i)}{\left(\sqrt{\sum_{i=1}^{N}(y_i - \overline{y}_i)^2}\right)\left(\sqrt{\sum_{i=1}^{N}(Y_i - \overline{Y}_i)^2}\right)} \tag{25}$$

$$MAE = \frac{1}{N}\sum_{i=1}^{n}|y_i - Y_i| \tag{26}$$

$$RMSE = \sqrt{\left(\frac{1}{N}\sum_{i=1}^{N}(y_i - Y_i)^2\right)} \tag{27}$$

Whereas the total number of data points is given by N, y_i is the actual or measured parameter value, $\overline{y}_i$ is the value of the mean for measured parameters, $\overline{Y}_i$ is the mean values of the predicted parameter, and values of the estimated parameter is Y_i [14,83]. During training, if the MAE and RMSE value approaches zero means that the model trained better. However, more emphasis is placed on the ability of the trained model to perform well when validated on the withheld testing data. Therefore, if the testing results (MAE and RMSE) approaches zero indicates the best performing model with an improved generalization capacity [23].

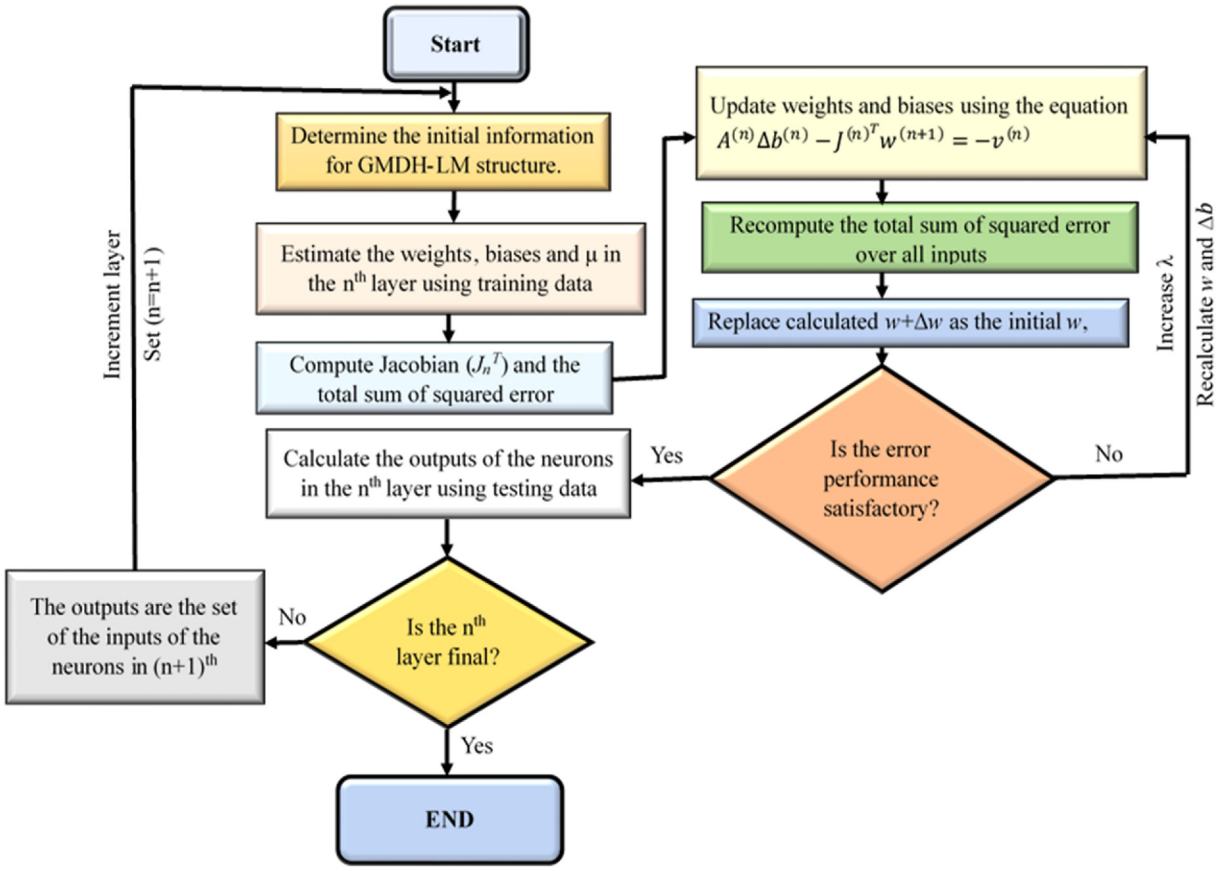

Fig. 4. Flowchart of the generalized structure for the GMDH-LM model.

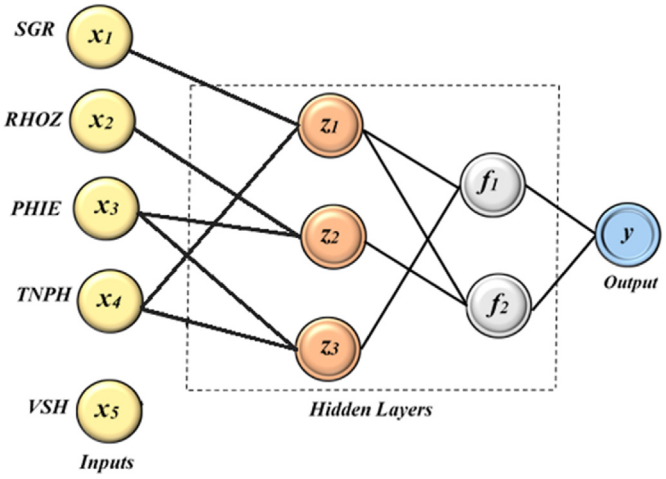

Fig. 5. Illustration of the proposed GMDH-LM neural network.

3.3. Statistical error analysis

The prediction results from the ANN model of BPNN when training with Well-1 and Well-2 data generated the mean absolute error (MAE) and root mean square error (RMSE) values of 0.025and 0.322 respectively Fig. 6. For Well-3 data which were used as Testing, the values obtained for MAE and RMSE were 0.026 and 0.753 respectively, as indicated in Fig. 7. Due to the non-linearity of the dataset, linear transfer function and hyperbolic tangent sigmoid were used for output and hidden layers of BPNN. Note that the quality output of the BPNN is highly dependent on the structure of the model that was obtained by a sequential trial and error process in this study. The optimal BPNN model structure observed after training was 5 inputs, a hidden layer with 8 neurons. From Fig. 6, the conventional GMDH permeability model achieved an error rate of 0.024 0.138 for training as MSE and MAE. During testing, the values achieved for MAE and RMSE were 0.690 and 0.049 respectively.

The best performing permeability model was GMDH-LM which trained well with its outcome having MAE and RMSE scores of 0.018 and 0.092 while generalizing better than conventional GMDH and BPNN on withheld data from Well-3 Fig. 7. During testing, GMDH-LM generated MAE and RMSE scores of 0.056 and 0.679 respectively. Based on a processing speed the GMDH-LM generated outcomes after 1.75 s of computational time, better than 2.06 s and 5.84 s which were used by conventional GMDH and BPNN respectively as expressed in Table 4.

On the other hand, the correlation coefficient (R) results for both training and testing indicate that GMDH-LM showed better permeability model performance than both conventional GMDH and BPNN models for both training and testing, Table 4.

3.4. Comparing with conventional GMDH and ANN

A comparison between the predicted and measured permeability for training is shown in Fig. 8 (a) GMDH-LM, Fig. 8 (b) conventional GMDH, and Fig. 8 (c) BPNN, for that of testing, is demonstrated in Fig. 9 (a) GMDH-LM, Fig. 9 (b) conventional GMDH, and Fig. 9 (c) BPNN. Both Figs. 8 and 9 show the scatter

Table 3
The proposed equations to predict Permeability.

Layers	Neurons	Equations
1	1 (Z_1)	$Z_1 = -32.9652 + 0.153768x_1 + 0.076551x_4 - 0.12999x_1^2 - 4.6E - 0.5x_4^2 + 0.002662x_1x_4$,
	2 (Z_2)	$Z_2 = 12.43097 + 0.120575x_2 - 0.123869x_3 - 0.0191x_2^2 - 0.06303x_3^2 + 0.054208x_2x_3$,
	3 (Z_3)	$Z_3 = -0.36839 + 0.511909x_3 - 0.835033x_4 - -0.00839x_3^2 - 0.0292x_4^2 + 0.0.000613x_3x_4$,
2	1 (f_1)	$f_1 = 409.0847 - 43.2289z_1 - 36.9531z_3 + 1.268331z_1^2 + 0.908063z_3^2 + 1.789357z_1z_3$,
	2 (f_2)	$f_2 = 58.70075 + 1.254165z_1 - 11.8796z_2 - 0.13131z_1^2 + 0.518262z_2^2 + 0.166494z_1z_2$,
Output (y)		$y = 67.4449 - 3.23016f_1 - 8.29554f_2 + 0.063436f_1^2 + 0.248207f_2^2 + 0.220129f_1f_2$.

diagram which correlates actual permeability values against the achieved results from GMDH-LM, conventional GMDH, and BPNN models. A tight cloud of data points about the diagonal line ($y = x$) for training and testing data assortments presents the high accuracy of the developed permeability models. Throughout the training process, GMDH-LM automatically learns the relationships which dominate structure variables. In this way, the optimum neuron structure generated is automatically selected in a manner that minimizes the values of the prediction error criteria and removes redundant neurons from the network which is the reason for a better sign of GMDH-LM model coherence. The performance of the developed predictive models for GMDH-LM, conventional GMDH, and BPNN is described as compared to the permeability data measured in Figs. 10 and 11.

3.5. Sensitivity analysis

To assign the relative importance of each active and effective well log on permeability prediction a sensitivity analysis was carried out. An analysis was conducted in all well logs. Sensitivity analysis results were shown in Fig. 12. Fig. 12 displays distributions and the contribution provided by each input well log in deciding permeability values of the predicted permeability against independent well logs. GMDH-LM model selected four well logs out of

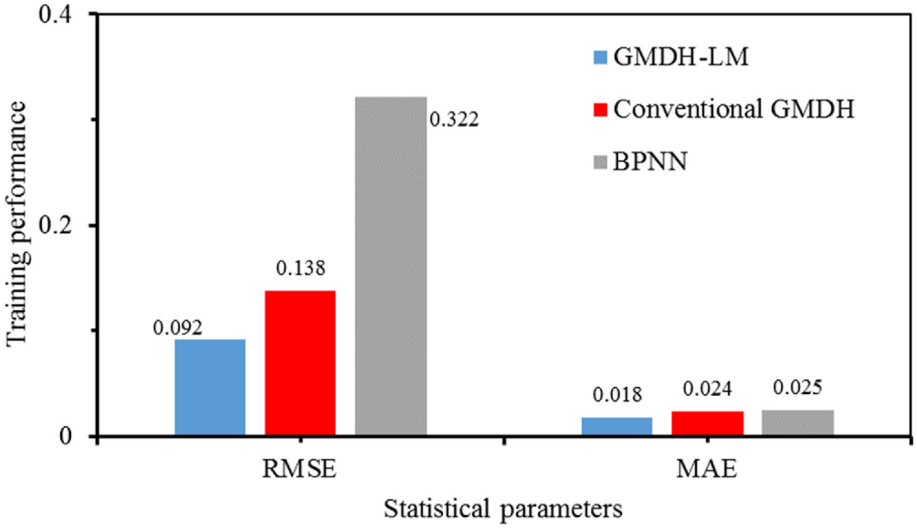

Fig. 6. Performance of GMDH-LM, conventional GMDH, and BPNN during training.

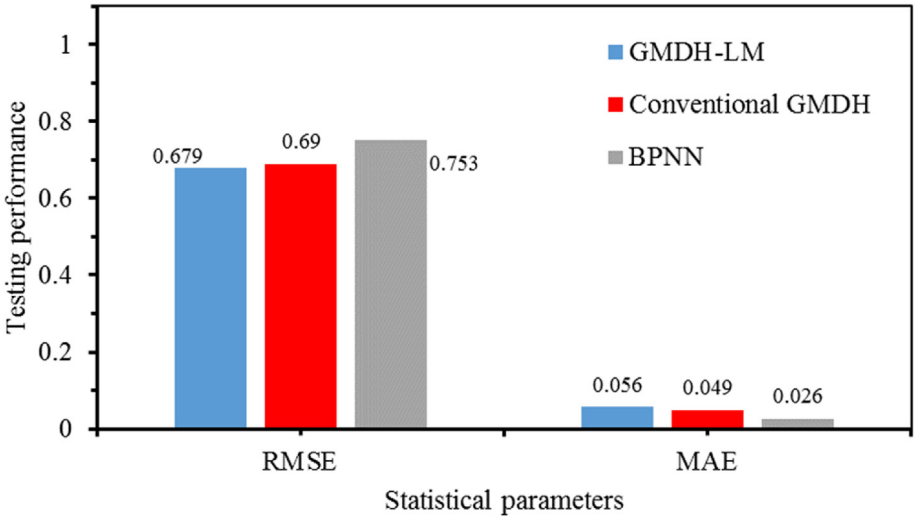

Fig. 7. Performance of GMDH-LM, conventional GMDH, and BPNN during testing.

Table 4
Statistical features of the permeability models developed.

Models	Training set			Testing set			Computational Time
	R	RMSE	MAE	R	RMSE	MAE	
GMDH-LM	0.9652	0.092	0.018	0.9252	0.679	0.056	1.75 s
Conventional GMDH	0.9541	0.138	0.024	0.9066	0.690	0.049	2.06 s
BPNN	0.9525	0.322	0.025	0.9015	0.753	0.026	5.84 s

the five inputs automatically, when estimating permeability. The Well logs selected by GMDH-LM were standard resolution formation density (RHOZ), effective porosity (PHIE), thermal neutron porosity (TNPH), and standard gamma-ray (SGR) logs. PHIE noted a significant contribution to permeability estimation with 3.92% likewise TNPH and SGR had a strong effect of 2.143% and 1.0%, respectively, RHOZ had less effect on the model of permeability estimation than all parameters with a value of 0.5%. Sensitivity analysis was conducted to analyze the contribution provided by each input well log to the determination of permeability values and was estimated by using Equation (28).

$$SA = \frac{1}{N}\sum_{i=1}^{N}\left(\frac{\delta Output\%}{\delta Input\%}\right)_i \times 100 \tag{28}$$

Whereas δoutput% is the percentage change of output and δinput% is the percentage change in the input. This implies that parameters change from a maximum to a minimum value. The lower the *SA*

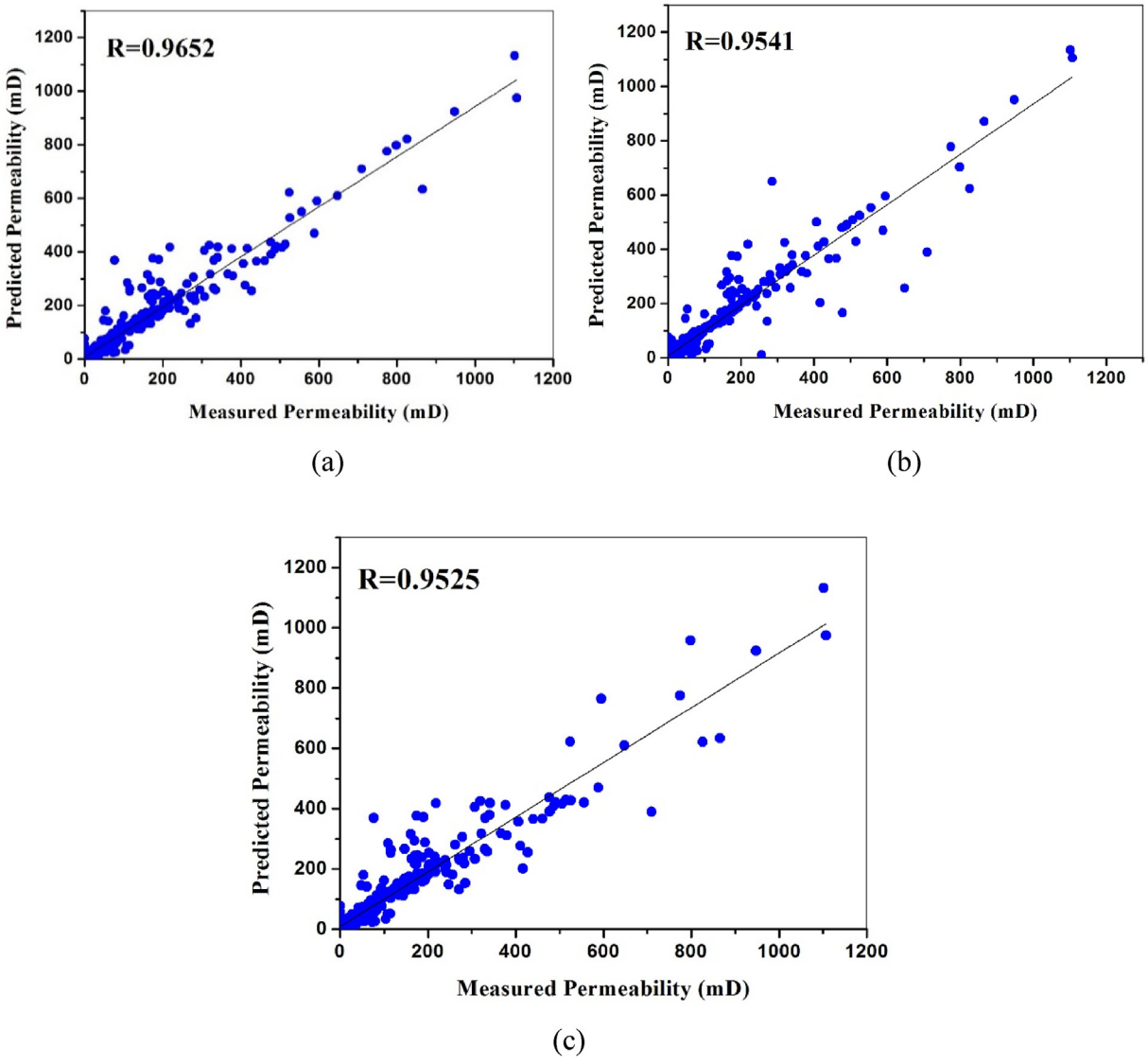

Fig. 8. The plot of the predicted value of permeability versus actual permeability for training set (a) GMDH-LM, (b) conventional GMDH, and (c) BPNN, permeability models.

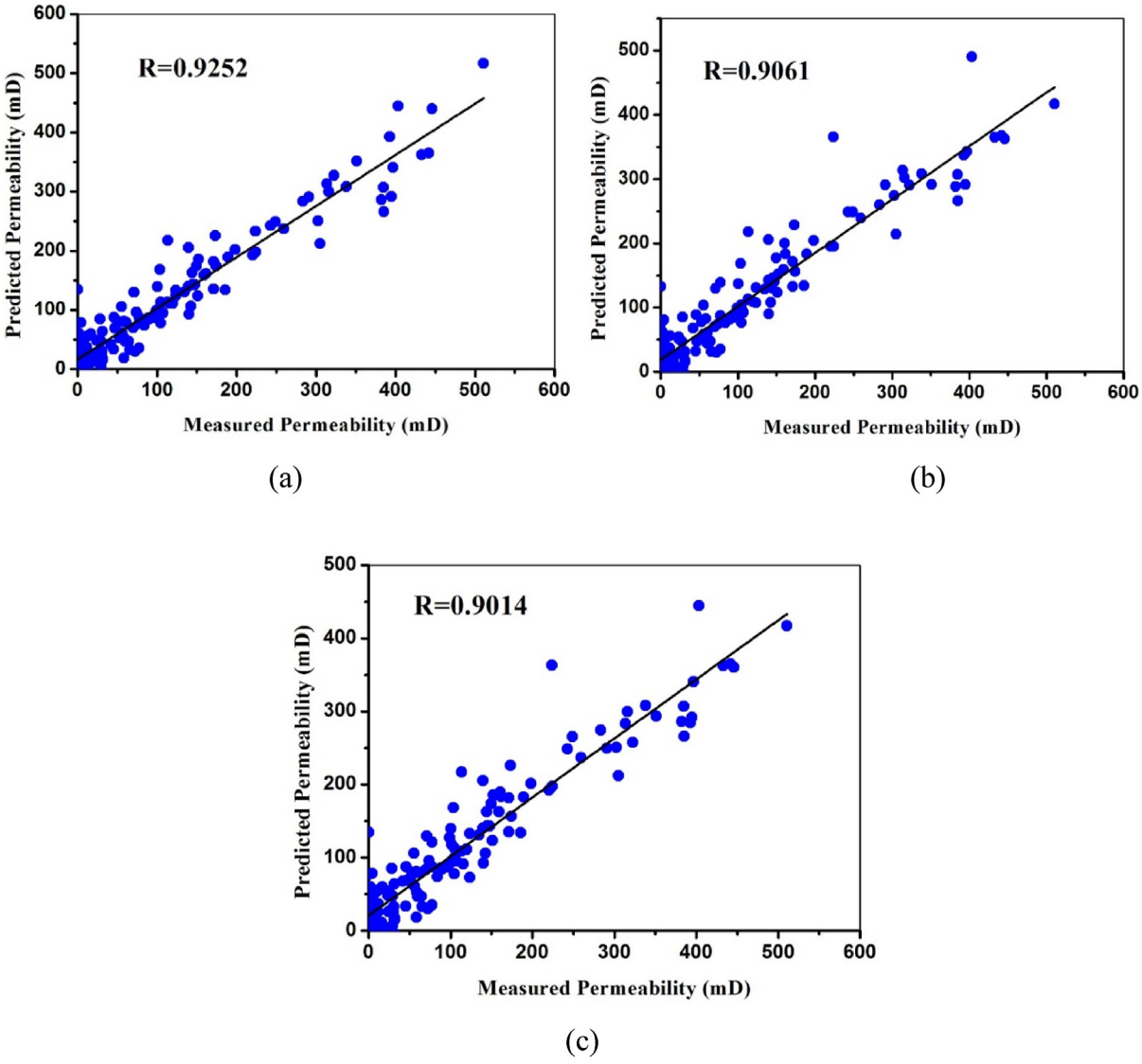

Fig. 9. The plot of the predicted permeability value versus actual permeability for the testing set for (a) GMDH-LM, (b) conventional GMDH, and (c) BPNN, permeability models.

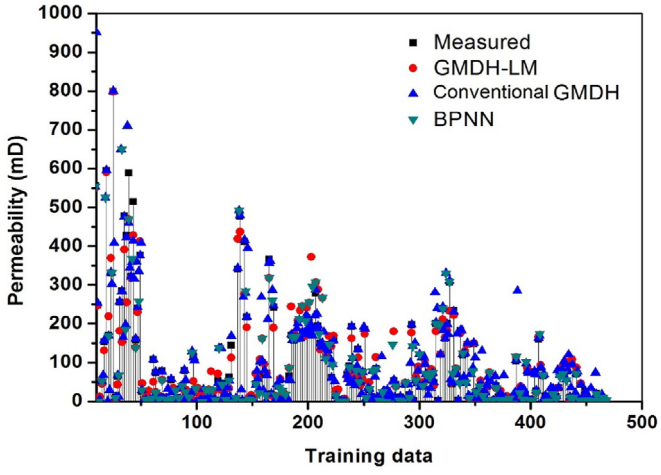

Fig. 10. GMDH-LM, BPNN, and conventional GMDH prediction in comparison with actual permeability for the training data set.

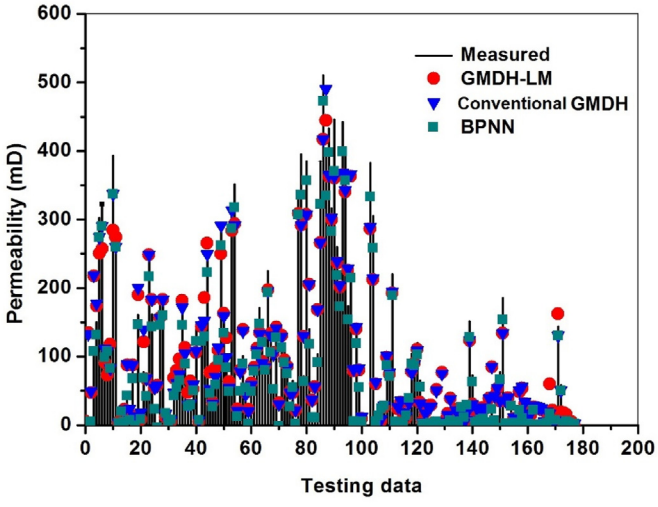

Fig. 11. Comparison of predicted permeability values of GMDH-LM, conventional GMDH, and BPNN with actual permeability for testing data set.

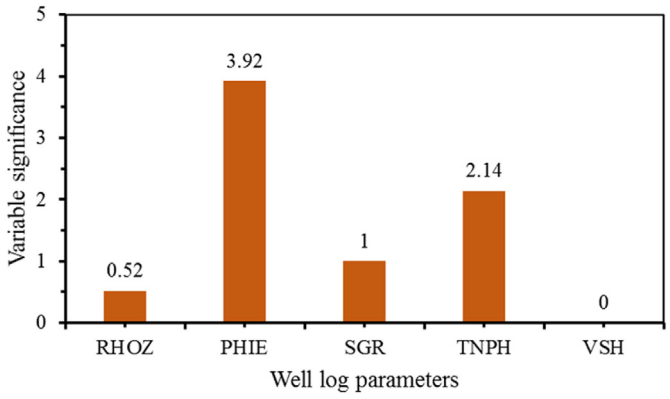

Fig. 12. Sensitivity analysis of the well log suite on the GMDH-LM permeability model.

value means that the input value has less effect on the generated permeability value while the higher value of SA indicates the well log parameter affected the predicted permeability outcome.

4. Conclusion

A sophisticated approach is required for a better estimation of reservoir permeability. Minor differences in expected outcomes contribute to time wastage and enormous investments. A minor change in estimation practices, on the other hand, may increase the value of the exploration project several times. Therefore, this study proposed an enhanced group method of data handling (GMDH) neural network by using a modified Levenberg-Marquardt algorithm as a means of offering an improved performance when predicting permeability from well logs. Well logs data from well-1 and well-2 of the West arm on the East Africa rift valley were considered as training data, while the predictivity of the models was judged on the data from well-3. In line with this, input parameters of a well log suite of TNPH, SGR, VSH, PHIE, and RHOZ, were used to develop the enhanced GMDH permeability model.

The results revealed that the GMDH-LM permeability model provided the least error margins with excellent training and testing capabilities than both conventional GMDH, and BPNN permeability models. The variable significance analysis was used to quantify the contribution of the individual well log on the permeability model performance. It was identified that SGR, TNPH, PHIE, and RHOZ produced significant contributions to the efficiency of the GMDH-LM permeability model.

The proposed concept of GMDH-LM in predicting permeability from well logs also comparable to conventional GMDH and ANN of BPNN techniques makes it a viable solution in attaining improved accuracy of permeability estimates. Therefore, based on the results of the present study, we can suggest GMDH-LM as an improved method to be considered as an alternative to the conventional GMDH for estimating permeability.

Author contributions

Chuanbo Shen: Overall supervision, Conceptualization, Funding, Resources, Writing – review & editing of the final manuscript. **Alvin K. Mulashani**: Conceptualization, Methodology, Software, Investigation, Writing – original draft, Writing – review & editing.**Baraka M. Nkurlu** Methodology, Software, Writing – review & editing. **Christopher N. Mkono**. Data curation, Software, Formal analysis, Writing – review & editing. **Martin Kawamala** Review writing and validation of the design model.

Declaration of competing interest

The authors declare that they have no known competing financial interests or personal relationships that could have appeared to influence the work reported in this paper.

Acknowledgments

This work was supported by the Major National Science and Technology Programs in the “Thirteenth Five-Year” Plan period (No. 2017ZX05032-002-004), the Outstanding Youth Funding of Natural Science Foundation of Hubei Province (No. 2016CFA055).

References

[1] Aydin G. Production modeling in the oil and natural gas industry: an application of trend analysis. Petrol Sci Technol 2014;32(5):555–64.
[2] Humbatova SI, Hajiyev NQO. Oil factor in economic development. Energies 2019;12(8):1573.
[3] Cantavella M. Fluctuations of oil prices and gross domestic product in Spain. Int J Energy Econ Pol 2020;10(2):57.
[4] Aydin G. Forecasting natural gas production using various regression models. Petrol Sci Technol 2015;33(15–16):1486–92.
[5] Teklu TW, Li X, Zhou Z, Abass H. Experimental investigation on permeability and porosity hysteresis of tight formations. SPE J 2018;23:672–90. 03.
[6] Sun H, Vega S, Tao G. Analysis of heterogeneity and permeability anisotropy in carbonate rock samples using digital rock physics. J Petrol Sci Eng 2017;156:419–29.
[7] Shen B, Wu D, Wang Z. A new method for permeability estimation from conventional well logs in glutenite reservoirs. J Geophys Eng 2017;14(5):1268–74.
[8] Xiong F, Sun W, Ba J, Carcione JM. Effects of fluid rheology and pore connectivity on rock permeability based on a network model. J Geophys Res: Solid Earth 2020;125(3) [no-no].
[9] Graczyk KM, Matyka M. Predicting porosity, permeability, and tortuosity of porous media from images by deep learning. Sci Rep 2020;10(1):1–11.
[10] Wójcik M, Kostowski W. Environmental risk assessment for exploration and extraction processes of unconventional hydrocarbon deposits of shale gas and tight gas: pomeranian and Carpathian region case study as largest onshore oilfields. J Earth Sci 2020;31(1):215–22.
[11] Kadhim ADFS, Imran M, Ahmed AL, Rasool MYF. Using NMR, core analysis, and well logging data to predict permeability of carbonate reservoirs: a case study. MS&E. 2020;671(1):012071.
[12] Rafik B, Kamel B. Prediction of permeability and porosity from well log data using the nonparametric regression with multivariate analysis and neural network, Hassi R'Mel Field, Algeria. Egyptian journal of petroleum 2017;26(3):763–78.
[13] Röding M, Ma Z, Torquato S. Predicting permeability via statistical learning on higher-order microstructural information. Sci Rep 2020;10(1):1–17.
[14] Ahmadi MA, Chen Z. Comparison of machine learning methods for estimating permeability and porosity of oil reservoirs via petro-physical logs. Petroleum 2019;5(3):271–84.
[15] Aljuboori FA, Lee JH, Elraies KA, Stephen KD. Using statistical approaches in permeability prediction in highly heterogeneous carbonate reservoirs. Carbonates Evaporites 2021;36(3):1–14.
[16] Erofeev A, Orlov D, Ryzhov A, Koroteev D. Prediction of porosity and permeability alteration based on machine learning algorithms. Transport Porous Media 2019;128(2):677–700.
[17] Zhu L-q, Zhang C, Wei Y, Zhang C-m. Permeability prediction of the tight sandstone reservoirs using hybrid intelligent algorithm and nuclear magnetic resonance logging data. Arabian J Sci Eng 2017;42(4):1643–54.
[18] Urang JG, Ebong ED, Akpan AE, Akaerue EI. A new approach for porosity and permeability prediction from well logs using artificial neural network and curve fitting techniques: a case study of Niger Delta, Nigeria. J Appl Geophys 2020;183:104207.
[19] Okon AN, Adewole SE, Uguma EM. Artificial neural network model for reservoir petrophysical properties: porosity, permeability and water saturation prediction. Modeling Earth Systems and Environment 2020:1–18.
[20] Aliouane L, Ouadfeul S-A, Djarfour N, Boudella A. Permeability prediction using artificial neural networks. A comparative study between back propagation and Levenberg–Marquardt learning algorithms. In: Mathematics of Planet Earth. Springer; 2014. p. 653–7.
[21] Santisukkasaem U, Olawuyi F, Oye P, Das DB. Artificial neural network (ANN) for evaluating permeability decline in permeable reactive barrier (PRB). Environmental Processes 2015;2(2):291–307.
[22] Thanh HV, Sugai Y, Sasaki K. Application of artificial neural network for predicting the performance of CO 2 enhanced oil recovery and storage in residual oil zones. Sci Rep 2020;10(1):1–16.
[23] Asante-Okyere S, Shen C, Yevenyo Ziggah Y, Moses Rulegeya M, Zhu X. Investigating the predictive performance of Gaussian process regression in

evaluating reservoir porosity and permeability. Energies 2018;11(12):3261.
[24] Ahmadi MA, Zendehboudi S, Lohi A, Elkamel A, Chatzis I. Reservoir permeability prediction by neural networks combined with hybrid genetic algorithm and particle swarm optimization. Geophys Prospect 2013;61(3):582–98.
[25] Moussa T, Elkatatny S, Mahmoud M, Abdulraheem A. Development of new permeability formulation from well log data using artificial intelligence approaches. J Energy Resour Technol 2018;140(7).
[26] Karimpouli S, Fathianpour N, Roohi J. A new approach to improve neural networks' algorithm in permeability prediction of petroleum reservoirs using supervised committee machine neural network (SCMNN). J Petrol Sci Eng 2010;73(3–4):227–32.
[27] Anifowose FA, Labadin J, Abdulraheem A. Ensemble model of non-linear feature selection-based extreme learning machine for improved natural gas reservoir characterization. J Nat Gas Sci Eng 2015;26:1561–72.
[28] Wang Y, Liu H, Yu Z, Tu L. An improved artificial neural network based on human-behaviour particle swarm optimization and cellular automata. Expert Syst Appl 2020;140:112862.
[29] Kaydani H, Mohebbi A. A comparison study of using optimization algorithms and artificial neural networks for predicting permeability. J Petrol Sci Eng 2013;112:17–23.
[30] Tian J, Qi C, Sun Y, Yaseen ZM, Pham BT. Permeability prediction of porous media using a combination of computational fluid dynamics and hybrid machine learning methods. Eng Comput 2020:1–17.
[31] Ascione F, Bianco N, De Stasio C, Mauro GM, Vanoli GP. Artificial neural networks to predict energy performance and retrofit scenarios for any member of a building category: a novel approach. Energy 2017;118:999–1017.
[32] Shen C, Asante-Okyere S, Yevenyo Ziggah Y, Wang L, Zhu X. Group method of data handling (GMDH) lithology identification based on wavelet analysis and dimensionality reduction as well log data pre-processing techniques. Energies 2019;12(8):1509.
[33] Nkurlu BM, Shen C, Asante-Okyere S, Mulashani AK, Chungu J, Wang L. Prediction of permeability using group method of data handling (GMDH) neural network from well log data. Energies 2020;13(3):551.
[34] Mulashani AK, Shen C, Asante-Okyere S, Kerttu PN, Abelly EN. Group method of data handling (GMDH) neural network for estimating total organic carbon (TOC) and hydrocarbon potential distribution (S1, S2) using well logs. Nat Resour Res 2021:1–18.
[35] Madala HR. Inductive learning algorithms for complex systems modeling. CRC press; 2019.
[36] Ivakhnenko A, Wunsch D, Ivakhnenko G. Inductive sorting-out GMDH algorithms with polynomial complexity for active neurons of neural network. Conference Inductive sorting-out GMDH algorithms with polynomial complexity for active neurons of neural network, vol. vol. 2. IEEE, p. 1169-1173.
[37] Ebtehaj I, Bonakdari H, Khoshbin F, Ab Ghani A, C Bong. Development of group method of data handling based on genetic algorithm to predict incipient motion in rigid rectangular storm water channel. Scientia Iranica Transaction A, Civil Engineering 2017;24(3):1000.
[38] Najafzadeh M, Barani G-A, Hessami-Kermani M-R. Evaluation of GMDH networks for prediction of local scour depth at bridge abutments in coarse sediments with thinly armored beds. Ocean Eng 2015;104:387–96.
[39] Menad NA, Noureddine Z, Hemmati-Sarapardeh A, Shamshirband S, Mosavi A, Chau K-w. Modeling temperature dependency of oil-water relative permeability in thermal enhanced oil recovery processes using group method of data handling and gene expression programming. Engineering Applications of Computational Fluid Mechanics 2019;13(1):724–43.
[40] Mesbah M, Habibnia S, Ahmadi S, Dehaghani AHS, Bayat S. Developing a robust correlation for prediction of sweet and sour gas hydrate formation temperature. Petroleum 2020. https://doi.org/10.1016/j.petlm.2020.07.007.
[41] Guo J, Wang H, Guo F, Huang W, Yang H, Yang K, et al. The back propagation based on the modified group method of data-handling network for oilfield production forecasting. J. Pet. Explor. Prod. Technol. 2019;9(2):1285–93.
[42] Mahdavi-Meymand A, Zounemat-Kermani M. A new integrated model of the group method of data handling and the firefly algorithm (GMDH-FA): application to aeration modelling on spillways. Artif Intell Rev 2020;53(4):2549–69.
[43] Amar MN, Larestani A, Lv Q, Zhou T, Hemmati-Sarapardeh A. Modeling of methane adsorption capacity in shale gas formations using white-box supervised machine learning techniques. J Petrol Sci Eng 2021:109226.
[44] Mahdaviara M, Rostami A, Shahbazi K. State-of-the-art modeling permeability of the heterogeneous carbonate oil reservoirs using robust computational approaches. Fuel 2020;268:117389.
[45] Youcefi MR, Hadjadj A, Boukredera FS. New model for standpipe pressure prediction while drilling using Group Method of Data Handling. Petroleum 2021. https://doi.org/10.1016/j.petlm.2021.04.003.
[46] Buryan P. Time series analysis by means of enhanced GMDH algorithm: Dissertation Thesis. CTU Prague; 2006.
[47] Hiassat M, Abbod M, Mort N, Hamparsum B. Using genetic programming to improve the GMDH in time series prediction. Statistical data mining and knowledge discovery 2003:257–68.
[48] Park H-S, Park B-J, Kim H-K, Oh S-K. Self-organizing polynomial neural networks based on genetically optimized multi-layer perceptron architecture. Int J Contr Autom Syst 2004;2(4):423–34.
[49] Oh S-K, Pedrycz W. Multi-layer self-organizing polynomial neural networks and their development with the use of genetic algorithms. J Franklin Inst 2006;343(2):125–36.
[50] Amin MF. Complex-valued neural networks: learning algorithms and applications. LAP LAMBERT Academic Publishing; 2018.
[51] Liang M, Zheng B, Zheng Y, Zhao R. A two-step accelerated Levenberg–Marquardt method for solving multilinear systems in tensor-train format. J Comput Appl Math 2021;382:113069.
[52] Fletcher A. Lithospheric Controls on the rifting of the Tanzanian Craton at the Eyasi rift. Eastern Branch of the East African Rift System; 2017.
[53] Scoon RN, Scoon RN, Steenbergen V. Geology of National Parks of Central/southern Kenya and northern Tanzania. Springer; 2018.
[54] Ring U. Tectonic dynamics in the African Rift valley and climate change. Oxford Research Encyclopedia of Climate Science; 2018.
[55] Maselli V, Kroon D, Iacopini D, Wade BS, Pearson PN, de Haas H. Impact of the East African Rift System on the routing of the deep-water drainage network offshore Tanzania, western Indian Ocean. Basin Res 2020;32(5):789–803.
[56] Simon B, Guillocheau F, Robin C, Dauteuil O, Nalpas T, Pickford M, et al. Deformation and sedimentary evolution of the Lake Albert rift (Uganda, east African Rift system). Mar Petrol Geol 2017;86:17–37.
[57] Shen C, Hu D, Min K, Yang C, Zeng X, Fu H, et al. Post-orogenic tectonic evolution of the jiangnan-xuefeng orogenic belt: insights from multiple geochronometric dating of the mufushan massif, south China. J Earth Sci 2020;31(5):905–18.
[58] Zhong Z, Carr TR, Wu X, Wang G. Application of a convolutional neural network in permeability prediction: a case study in the Jacksonburg-Stringtown oil field, West Virginia, USA. Geophysics 2019;84(6):B363–73.
[59] Mueller AV, Hemond HF. Extended artificial neural networks: incorporation of a priori chemical knowledge enables use of ion selective electrodes for in-situ measurement of ions at environmentally relevant levels. Talanta 2013;117:112–8.
[60] Jia W, Zhao D, Shen T, Ding S, Zhao Y, Hu C. An optimized classification algorithm by BP neural network based on PLS and HCA. Appl Intell 2015;43(1):176–91.
[61] Li S, Li S, Zhao H, An Y. Design and implementation of state-of-charge estimation based on back-propagation neural network for smart uninterruptible power system. Int J Distributed Sens Netw 2019;15(12). 1550147719894526.
[62] Cahyadi TA, Syihab Z, Widodo LE, Notosiswoyo S, Widijanto E. Analysis of hydraulic conductivity of fractured groundwater flow media using artificial neural network back propagation. Neural Comput Appl 2021;33:159–79.
[63] Du B, Lund PD, Wang J. Combining CFD and artificial neural network techniques to predict the thermal performance of all-glass straight evacuated tube solar collector. Energy 2020:119713.
[64] Konaté AA, Pan H, Khan N, Ziggah YY. Prediction of porosity in crystalline rocks using artificial neural networks: an example from the Chinese continental scientific drilling main hole. Studia Geophys Geod 2015;59(1):113–36.
[65] Pereira IM, Moraes DA. Monitoring system for an experimental facility using GMDH methodology. Brazilian J. Radiat. Sci. 2021;8(3B).
[66] Köne AÇ, Büke T. Forecasting of CO2 emissions from fuel combustion using trend analysis. Renew Sustain Energy Rev 2010;14(9):2906–15.
[67] Hosseini SA, Taheri B, Abyaneh HA, Razavi F. Comprehensive power swing detection by current signal modeling and prediction using the GMDH method. Protection and Control of Modern Power Systems 2021;6(1):1–11.
[68] Duan W, Congress SSC, Cai G, Liu S, Dong X, Chen R, et al. A hybrid GMDH neural network and logistic regression framework for state parameter-based liquefaction evaluation. Can Geotech J 2021;(ja).
[69] Dorn M, Braga AL, Llanos CH, Coelho LS. A GMDH polynomial neural network-based method to predict approximate three-dimensional structures of polypeptides. Expert Syst Appl 2012;39(15):12268–79.
[70] Bueno EI, Pereira IM. GMDH and neural networks applied in monitoring and fault detection in sensors in nuclear power plants. 2011.
[71] Farlow SJ. Self-organizing methods in modeling: GMDH type algorithms. CrC Press; 2020.
[72] Hemmati-Sarapardeh A, Hajirezaie S, Soltanian MR, Mosavi A, Nabipour N, Shamshirband S, et al. Modeling natural gas compressibility factor using a hybrid group method of data handling. Engineering Applications of Computational Fluid Mechanics 2020;14(1):27–37.
[73] Teng G, Xiao J, He Y, Zheng T, He C. Use of group method of data handling for transport energy demand modeling. Energy Science & Engineering 2017;5(5):302–17.
[74] Yu H, Wilamowski BM. Levenberg-marquardt training. Industrial electronics handbook 2011;5(12):1.
[75] Lin Y, O'Malley D, Vesselinov VV. A computationally efficient parallel L evenberg-M arquardt algorithm for highly parameterized inverse model analyses. Water Resour Res 2016;52(9):6948–77.
[76] Gavin HP. The Levenberg-Marquardt algorithm for nonlinear least squares curve-fitting problems. Department of Civil and Environmental Engineering; 2019. p. 1–19. Duke University http://people duke edu/~ hpgavin/ce281/lm pdf.
[77] Naveen M, Jayaraman S, Ramanath V, Chaudhuri S. Modified Levenberg Marquardt algorithm for inverse problems. Conference Modified Levenberg Marquardt algorithm for inverse problems. Springer, p. 623-632.
[78] Yang K, Jiang G-H, Peng H-F, Gao X-W. A new modified Levenberg-Marquardt algorithm for identifying the temperature-dependent conductivity of solids based on the radial integration boundary element method. Int J Heat Mass Tran 2019;144:118615.

[79] Fletcher R. A modified Marquardt subroutine for non-linear least squares. 1971.
[80] Yang X. A higher-order Levenberg–Marquardt method for nonlinear equations. Appl Math Comput 2013;219(22):10682–94.
[81] Cui M, Yang K, Xu X-l, Wang S-D, Gao X-W. A modified Levenberg–Marquardt algorithm for simultaneous estimation of multi-parameters of boundary heat flux by solving transient nonlinear inverse heat conduction problems. Int J Heat Mass Tran 2016;97:908–16.
[82] Elkatatny S, Mahmoud M, Tariq Z, Abdulraheem A. New insights into the prediction of heterogeneous carbonate reservoir permeability from well logs using artificial intelligence network. Neural Comput Appl 2018;30(9):2673–83.
[83] Adeniran AA, Adebayo AR, Salami HO, Yahaya MO, Abdulraheem A. A competitive ensemble model for permeability prediction in heterogeneous oil and gas reservoirs. Applied Computing and Geosciences 2019;1:100004.